ANEXO 6

Patarroyo ME, **Alba MP**, Reyes C, Rojas-Luna R, Patarroyo MA. The Malaria Parasite's Achilles' Heel: Functionally-relevant Invasion Structures. Curr. Issues. Mol. Biol. 2015. 18:11-20.

The Malaria Parasite's Achilles' Heel: Functionally-relevant Invasion Structures

Manuel E. Patarroyo [1,2,*], Martha P. Alba[1,3], Cesar Reyes[1], Rocio Rojas-Luna[1], and Manuel A. Patarroyo[1,3]

[1]Fundación Instituto de Inmunología de Colombia (FIDIC), Bogotá, Colombia
[2]Universidad Nacional de Colombia, Bogotá, Colombia
[3]Universidad del Rosario, Bogotá. Colombia
*Corresponding author: Tel: 57-1-2225277 E-mail: mepatarr@gmail.com

Abstract
Malaria parasites have their Achilles' heel; they are vulnerable in small parts of their relevant molecules where they can be wounded and killed. These are sporozoite and merozoite protein **c**onserved **h**igh **a**ctivity **b**inding **p**eptides (cHABPs), playing a critical role in binding to and invasion of host cells (hepatocytes and erythrocytes, respectively). cHABPs can be modified by specific amino acid replacement, according to previously published physicochemical rules, to produce analogues (mHABPs) having left-handed polyproline II ($PPII_L$)-like structures which can modulate an immune response due to fitting perfectly into the HLA-DRβ1* peptide binding region (PBR) and having an appropriate presentation to the T-cell receptor (TCR).

Achilles' heel of microbes
According to the historian Statius, the Nereid Thetis, Achilles' mother dipped him headfirst into the River Styx when he was born to make him immortal and so that no arrow could wound him; not having anywhere else to hold him by, she held him by his right heel, this therefore becoming the only vulnerable site for the hero of the Iliad.
Microbes also have their Achilles' heel, particularly the parasite *P. falciparum,* the causal agent of the lethal form of malaria; the **c**onserved **h**igh **a**ctivity **b**inding **p**eptides (cHABPs) from sporozoite (Spz) and merozoite (Mrz) proteins directly participate in binding to and invasion of host cells (hepatocytes and erythrocytes, respectively) (Garcia et al., 2006; Rodriguez et al., 2008). These conserved functionally relevant sequences, common to all the parasite's genetic variants in the world, are highly vulnerable to blocking parasite cell binding, cell lysis and death. When properly modified, these structures become mHABPs (Patarroyo and Patarroyo, 2008; Curtidor et al., 2011; Patarroyo et al., 2011) containing segments similar to native protein structures while some other portions, modified according to previously demonstrated physicochemical rules, allow their fit into the HLA-DRβ1* **p**eptide **b**inding **r**egion (PBR), converting mHABPs into strain-transcending, **i**mmune **p**rotection-**i**nducing **s**tructures (IMPIPS). IMPIPS induce very high, strong, specific antibody and protective immune responses, as has been thoroughly demonstrated, establishing a new methodology for vaccine development. These cHABPs are thus the Achilles' heel of microbes, particularly the malaria parasite.

The malaria parasite's Achilles' heel revealed by 3D structural analysis
Analysing the Spz proteins studied CSP region I cHABP 4383 contains the RxLxE ***P****lasmodium falciparum* **ex**port **el**ement (PEXEL) motif (shadowed) (Table 1) (Hiss et al., 2008) mediating parasite protein membrane transport and Kappa B factor activation to induce Spz differentiation into Mrz. CSP 4388 (Table 1), considered to link repeats region to RII was localized 15 residues upstream the high content **h**eparan **s**ulphate **p**roteo**gly**can (HSPG) binding site on hepatocytes where the parasite will become arrested and reproduce (Mota et al., 2001; Sibley, 2004). This CSP region I 3D structure has not yet been determined, therefore, these cHABP localizations are not shown in Figure 1. However, the 3D structure for the C-terminal CSP region III (named the α **t**hrombo**s**pondin **r**elated (TSR) domain containing highly polymorphic T-helper epitopes Th2R, Th3R and CS.T3 has recently been determined by X-ray crystallography (Doud et al., 2012), an unexpected folding being found where the N and C termini are extremely close to each other. Intermediate conserved binding capacity peptide 4397 (Figure 1A, Table 1) in the β1 strand of this structure establishes a network of H-bonds between ^{323}I and ^{333}P with ^{319}Y from 4394, ^{324}Q with ^{355}K, ^{328}S with ^{346}I, in non-binding 4400 and 4398 peptides respectively, and ^{341}G with ^{369}C in highly variable non-binding sequence 4403 (J. E. Suarez et al., 2001). The CS.T3 conserved region associated with CD4* T-cell response in our 4405 peptide does not bind to hepatocytes. Sporozoite TRAP cHABP 3243 (Table 1) plays a main role in cell entry, cHABP 3271 (Table 1) contains the residues forming the metal ion-dependent adhesion site (MIDAS, highlighted) and 3279 (Figure 1B) which is the HSPG binding site located in the vWA domain (Pihlajamaa et al., 2013). It was also seen that bridges are formed between intermediate binding peptide 3277 (Figure 1B) amino acids ^{201}F, ^{202}L, ^{203}V and ^{205}C with ^{197}A, ^{198}F, ^{199}N and ^{200}R (Figure 1B). Similarly, cHABP 3287 (Figure 1C) located in the TSR region formed by one ripped and two anti-parallel and β-strands forms a groove conformed by π cation interactions between ^{247}W, ^{250}W and ^{262}R, ^{264}R (respectively), plus 3 H-bonds established between cHABP 3289 ^{243}S, ^{248}D and ^{251}S with ^{266}R, ^{263}S and ^{264}R (Figure 1C). Positively-charged residues from this structure bind to negatively-charged receptors like **h**eparan **s**ulphate **p**roteo**g**lycans (HSPG) from hepatocytes and endothelial cells (Tossavainen et al., 2006) for mediating cell traversal activity and invasion. Meanwhile, TRAP 3347 (^{541}Y**A**GEPAP**F**VEPLGEE^{555}) located 15 residues upstream the aldolase binding site, mediates this protein's binding to

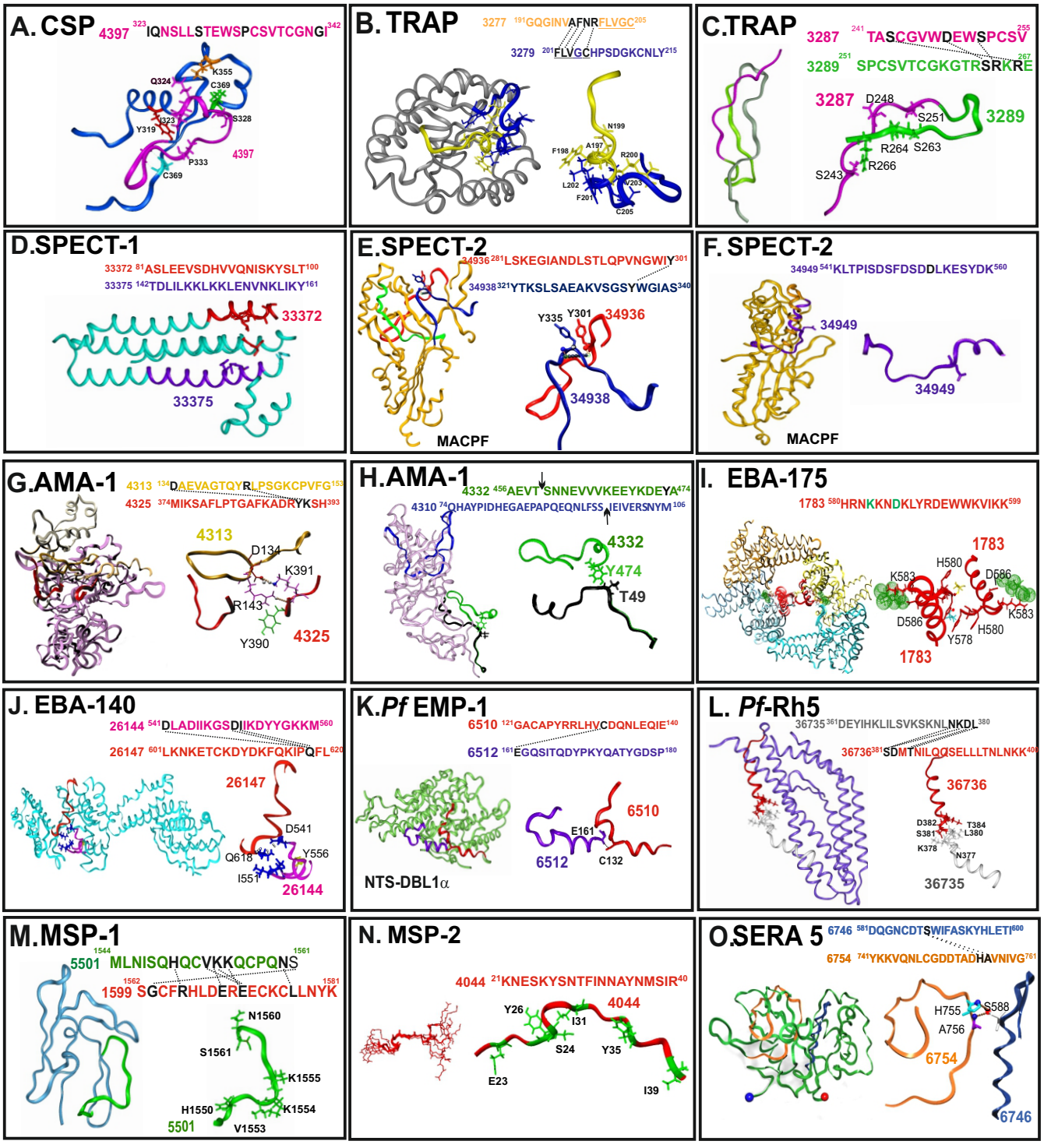

Figure 1. 3D structure ribbon representation of malarial proteins (determined by X-crystallography) displaying cHABP localization and (on the right-hand side) isolated cHABPs establishing H-bonds amongst themselves to create the niche, trough, channel or cavity where receptors bind. (**A**). CSP the C-terminal region III (PDB 3VDK) (Doud et al., 2012). (**B**). TRAP vWA domain (PDB 4F1J) (Pihlajamaa et al., 2013). (**C**) TRAP TSR domain (PDB 2BBX) (Tossavainen et al., 2006). (**D**) SPECT-1 protein (PDB 4U5A) (Hamaoka and Ghosh, 2014). (**E** and **F**) SPECT-2 C8α-MACPF domain (PDB 2QQH) (Hadders et al., 2007). (**G**) *P. falciparum* AMA-1 (PDB 1Z40) (Bai et al., 2005). (**H**) *P. vivax* AMA-1 (PDB 1W81) (Pizarro et al., 2005). (**I**) EBA-175 RII dimeric fragment (PDB 1ZRO) (Tolia et al., 2005). (**J**) EBA-140 protein (PDB 4JNO) (Lin et al., 2012). (**K**) Pf EMP-1 DBL1α domain (PDB 2XU0) (Juillerat et al., 2011). (**L**) Pf Rh5 (PDB 4WAT) (Chen et al., 2014). (**M**) MSP-1 19kDa fragment (PDB 1OB1) (Pizarro et al., 2003). (**N**) MSP-2 1H-NMR 3D structure cHABP 4044 structure; dodecylphosphocholine-2H38 (DPC) binding residues shown in green. (**O**) SERA-5 fragment (PDB 3CH2) (Hodder et al., 2009).

Table 1. Peptides having *gauche*+ and *gauche*- conformation. Amino acid sequences for *P. falciparum* Spz and Mrz cHABPs (their critical binding residues are shown in bold) and their corresponding mHABPs below (in bold), with their critical binding and replaced residues highlighted in bold. The same amino acids in their corresponding peptide analogues are represented by a dashed line. Colors in the Table show the HLA-DRβ1* PBR register region (pink) and structural features (green). mHABPs' reciprocal antibody titers were determined by IFA (shown in brackets). Prot indicates total number of protected *Aotus* after experimental challenge. DR: HLA-DRβ1* allele with which each HABP experimentally displayed high HLA-DRβ1* purified molecule binding capacity. Peptide ***24238** having *gauche*– orientation. ND: not determined by Spz challenge due to weird and non-reproducible results obtained with the only *Aotus* monkey-adapted *P. falciparum* strain (Santa Lucia).

Peptides with *gauche*+ conformation

	Peptide	Sequence	3D Structure	II	III	Prot	DR	
CSP	4383	NSRSLGENDDGNNEDNEKLR	Random	0	0			
	25608	K--F-----PNA-P	Classical β–Turn type II P10-N13	2(2560)	2(2560)	ND	4	
	4388	GNGQGHNMPNDPNRNVDENA	Random	0	0			
	32958	-----L--N-P--F-----	Classical β–Turn type I N15-E18	2(640)	3(1280)	ND	4	
	4397	IQNSLSTEWSPCSVTCGNGI	ND	ND	ND	ND		
TRAP	3243	YLVNGRDVQNNIVDE	Random by CD	0	0	ND		
	24312	DLFH-----TM-----NKY	Random by CD	2(320)	2(320)	ND	11	
	3271	TDGIPDSYQDSLKES	3_{10}–Helix Y8-S11	ND	ND	ND		
	3277/3279	VAFNRYLVGCHPSDGKCNLY	Random	0	0	ND		
	24238	----FH--T--AP--T---	Classical β–Turn type III A2-R5	2(1280)	2(1280)	ND	7	*
	3287/3289	TASCGVWDEWSPCSVTCGKGTRS	Random by CD	0	0	ND		
	24242	-------V-TAV-M----RK	Random	2(1280)	2(1280)	ND		
	3289	SPCSVTCGKGTRSRK	Distorted β–Turn type III'G8-T11	0	0	ND		
	24246	--T---V---AF-F-RE	Classical β–Turn type III' T6-K9	1(1280)	1(1280)	ND		
SPECT-1	33375	TDLILKKLKKLENVNKLIKY	α–Helix L8-L17	0	0	ND		
	38150	----A-G--Q-T--	α–Helix by CD	2(320)		ND	11	
SPECT-2	34938	YTKSLSAEAKVSGSYWGIAS	Random	0	0	ND		
	38890	SD---A-A--------	α–Helix by CD	1(320)	1(640)	ND		
	34949	KLTPISDSFDSDDLKESYDK	Distorted α–Helix S6-F9			ND		
	38128	----------T-----	α–Helix by CD	1(320)	1(640)	ND		
	34959	CVDTTIWSGVNNLSLVALDG	α–Helix by CD	0	0	0/5		
	38976	-----H-----	α–Helix by CD	2(1280)	2(1280)	ND		
AMA-1	4310	QHAYPIDHEGAEPAPQEQNL	Random by CD	ND	ND	ND		
	4313	DAEVAGTQYRLPSGKCPVFG	Random	0	0	0/5		
	10022	------FH----S---	Distorted β–Turn type III' T7-F10	0	1(5120)	1/5	β5*1	
	4325	MIKSAFLPTGAFKADRYKSH	β–Turn and short α–Helix K13-R16	0	0	0/5	3,11	
	13486	---AS-D------SP-----	α–Helix by CD	3(2560)	2(1280)	2/5	ND	
	4332	AEVTSNNEVVVKEEYKDEYA	Random by CD	0	0	0/5		
	37940	---------Q---V--QF-D	α–Helix by CD	1(160)	1(80)	ND		
EBA-175	1783	HRNKKNDKLYRDEWWKVIKK	α–Helix N6-K20	0	0	0/5	3,11	
	22814	----M-Y--T---DVW	α–Helix K3-K11	2(5120)	ND	2/10	15	
EBA-140	26147	LKNKETCKDYDKFQKIPQFL	Random	0	0	0/6		
	36620	------T--M----DS--	α–Helix by CD	1(320)	1(320)	ND		
Pf-EMP-1	6510	GACAPYRRLHVCDQNLEQIE	α–Helix by CD	ND	ND	ND		
	24196	--T-D-F--L-TP---	α–Helix by CD	1(320)	2(160)	2/10	4	
SERA-5	6746	DQGNCDTSWIFASKYHLETI	α–Helix by CD	0	0	0/5	3,11	
	23230	-SI-A--R----L----	α–Helix N2-K12	1(320)	ND	1/9	3	
	6754	KKVQNLCGDDTADHAVNIVG	Random	0	0	0/6		
	23426	--T------L-T----	Classical β–Turn type V V3-L6	3(320)	ND	1/9	4	
MSP-2	4044	KNESKYSNTFINNAYNMSIR	Classical β–Turn type III S7-F10	0	0	0/5		
	10008	-----EV------	Distorted β–Turn type III Y6-T9 and A14-M17	2(5120)	1(5120)	1/3	12	
Pf-RH-5	36727	GKYIAVDAFIKKINETYDKV	α–Helix by CD	0	0	0/6		
	38940	---R--M--V--Q--KSK	ND	0	2(160)	ND	11	

Peptides with *gauche*- conformation

MSP-1	5501	MLNISQHQCVKKQCPQNS	Random	0	0	0/5	7	
	24148	---ML-T-MMMT--K	Short α–Helix S5-V10	2(2560)	ND	2/8	7	
AMA-1	4313	DAEVAGTQYRLPSGKCPVFG	Random	0	0	0/5		
	13480	------WF-----S---	Distorted β–Turn type III' T7-F10	2(640)	2(320)	0/5	11	

the actin-myosin motor of apicomplexa which are critical for Spz motility (Sultan et al., 1997).

The very recently described SPECT-1 3D structure (Hamaoka and Ghosh, 2014) provides very strong support for our findings, since hypothetical RBC membrane cholesterol molecule (630 $Å^3$) could fit in such very spacious interior cavity having around 750 $Å^3$. cHABPs 33372 and 33375 are components of this cavity (Figure 1D, Table 1). On the other hand, cHABPs 33375 and 33374 (^{122}LISNLSKRQQKLKGDKIKKV^{141}) established H-bonds between themselves.

SPECT-2 containing a 40kDa membrane attack complex pore forming (MACPF) domain or cholesterol-dependent cytolysins (CDC) (Gilbert et al., 2014) is formed by D1, D2, D3 and D4 domains, where D4 binds to the cell membrane and D2 binds to D1 and D3 to mediate insertion into the membrane and pore formation (Hadders et al., 2007). A series of important cHABPs are found in the (MACPF) domain, such as cHABP 34938 (Table 1) and 34936, establishing H-bonds via ^{335}Y with ^{301}Y (Figure 1E) to generate a niche where a still unrecognized receptor binds to mediate cell traversal activity. By contrast, SPECT-2 34949 cHABP in D3 (Figure 1F, Table 1) (Hadders et al., 2007) interacts with heparin-like and chondroitin sulphate receptors on cells. After alignment with the complement component C8 alpha chain, it was found that ^{552}D (34949) is involved in oligomerisation of perforin due to its negative charge and location (Baran et al., 2009). SPECT-2 cHABP 34959 (Table 1) outside the MACPF domain contains the ^{744}TTL(I)Y^{747}(W) cholesterol binding motif on membrane surface (Farrand et al., 2010) which is critical in pore formation and cell traversal activity.
STARP 20546 (^{41}VIKHN**RF**L**SE**YQSNFLGGGY^{60}) displays the PEXEL motif RxLxE (shadowed), suggesting this protein is transported from the micronemes to the Spz membrane where it can be identified by immunofluorescence (Bermudez et al., 2010).

Regarding **Mrz invasion of RBC**, the thoroughly analyzed AMA-1 protein, deeply involved in Mrz reorientation, moving junction formation and parasitophorous vacuole resealing during RBC invasion (Yap et al., 2014), cHABPs 4313 (Table 1) in domain I and 4325 (Table 1) in domain II of this protein form the niche or trough via H-bonds between ^{134}D and ^{143}R with ^{390}Y and ^{391}K where a still unrecognized receptor binds (Bai et al., 2005) (Figure 1G). A very informative finding for invasion of host cells was shown by the H-bond established between ^{49}T some residues downstream AMA-1 cHABP 4310 (Table 1) localized in this molecule's prodomain and ^{474}Y in cHABP 4332 (Table 1) localized 450 residues downstream cHABP 4310 in domain III, containing this molecule's cleavage site (arrow) (Figure 1H). After cleavage, cHABP 4332 remains anchored to the Spz membrane and is the only cHABP found inside infected RBC, demonstrating different domains' functional compartmentalization and cooperation to perform a set function (4313 and 4325 involved in RBC invasion present in domains I and II, respectively; and 4310 and 4332 in the prodomain and domain III, respectively, involved in hepatocyte invasion).
Concerning the most relevant of the Duffy binding-like (DBL) family of proteins (McHenry and Adams, 2006) binding to neuraminidase sensitive receptors EBA-175 ^{583}K and ^{586}D, mHABP 1783 (^{580}**H**RN^{583}**K**KN^{586}**D**KLYRDE**W**^{594}**W**K^{596}**V**IKK^{599}) bind to glycophorin A receptor glycan 5 on RBC while ^{594}W induces fold stabilization and ^{580}H establishes H-bonds with its contralateral ^{596}V to allow the dimerization of this protein to mediate RBC attachment and invasion (Tolia et al., 2005; Ambroggio et al., 2013) (Figure 1I). EBA-175 cHABPs 1815 (^{1220}YTNQ**NI**NISQERDLQKHG FH^{1239}) and 1818 (^{1280}NNNFNNIPSR**Y**NLY**D**K**K**LDL^{1299}) are located in regions IV–V of this protein and antibodies against this region neutralize multiple *P. falciparum* strains *in vitro* (Ambroggio et al., 2013); however, no 3D structure has been determined so far for EBA-175 regions IV-V.

In another member of the DBL family, cHABP 26147 (Table 1) from the relevant EBA-140 protein (which also binds to neuraminidase sensitive receptor) establishes three H-bonds via ^{618}Q with cHABP 26144 ^{541}D, ^{550}D and ^{551}I, the latter exposing the α-helix where ^{556}Y interacts with the acetamide group in sialic acid in RBC glycophorin C (Figure 1J) (Lin et al., 2012).

Regarding another member of this DBL family, cHABP 6510 (Table 1) from *Pf*-EMP-1, expressed on infected erythrocyte (iE) membrane, establishes an H-bond between ^{132}C and ^{161}E in cHABP 6512 (Patarroyo et al., 2014) (Figure 1K), forming the niche where the A1 blood group terminal α-1,3 linked N-acetylgalactosamine (Vigan-Womas et al., 2012) binds through residues ^{138}Q and ^{140}E in cHABP 6510 to form rosettes with non-infected erythrocytes binding to small vessel endothelial cells to induce severe placental and cerebral malaria.

The *Pf*-RH5 protein, a member of the erythrocyte binding ligand (EBL) family, mediates a critical non-redundant interaction with human RBC surface protein basigin (present in other tissues) during invasion (Crosnier et al., 2011; Wright et al., 2014). cHABP 36735 amino acids ^{377}N, ^{378}K, ^{379}D and ^{380}L interact with cHABP 36736 ^{381}S, ^{382}D and ^{384}T by H-bond formation (Figure 1L) to create a niche where RBC bind and where a single amino acid replacement determines the preference for *Aotus* or human RBC binding.

MSP-1 cHABP 5501 (Table 1) located in this molecule's 19 kDa fragment N-terminus and being the only one found inside iE, has a highly complex H-bond network between ^{1550}H, ^{1553}V, ^{1554}K, ^{1555}K, ^{1560}N and ^{1561}S with 1599 ^{1563}G, ^{1566}R, ^{1570}E, ^{1572}E, and ^{1577}L the neighboring non-binding-peptide (Figure 1M) (Patarroyo et al., 2010b).

In the very relevant and most abundant protein on Mrz surface, MSP-2 mHABP 4044 (Table 1) binds via ^{23}E, ^{24}S, ^{26}Y, ^{31}I, ^{35}Y, ^{39}I to RBC membrane phosphocholine (determined by isotope-labeled dodecylphosphocholine) moiety recognized by ^{1}H-NMR (Zhang et al., 2008) (Figure 1N).

SERA-5 cHABP 6754 (Table 1) forms H-bonds via ^{755}H and ^{756}A with 6746 (Table 1) ^{588}S, forming the non-canonical enzymatic triad (Figure 1O) for this relevant molecule in malarial protein processing and egress (Hodder et al., 2009). No function has been assigned yet for SERA 6737 (^{401}YD**NI**L**V**K**M**F**K**T**NE**NNDKSEL**I**^{421}) but it is located 20 residues downstream the cleavage site of this protein during Mrz and Spz maturation and processing by subtisilin 1 (Kanodia et al., 2014), suggesting it is only exposed after SERA processing.

HRPII 6800 (^{1}Y**N**NSAF**NN**NLCSKNA**K**GLNLN^{21}), one residue upstream this protein's PEXEL motif, is deeply involved in protein trafficking and HRPII 6800 exposure on iE membrane (Boddey et al., 2009).

Achilles can also die

All the foregoing, striking data clearly shows that invasion by *P. falciparum* Spz and Mrz requires this parasite to create a niche, trough, channel or cavity formed by one or two cHABPs localized in different molecule regions or domains for binding to the receptors on host cells (Patarroyo et al., 2010a). These cHABPs, due to their critical function during infection, cannot display variations in their amino acid sequences or in their 3D structure, therefore being immunologically silent and making them the malaria parasite's Achilles' heel.

Consequently, these cHABPs are excellent targets for inducing a protective, strain-transcending immune response to impede, block or destroy parasite function.

When some critical host cell binding residues in cHABPs have been appropriately modified (mHABP) as determined by glycine analogue scanning, their altered structures allow them to fit into the HLA-DRβ* PBR. This makes them high specific antibody titer inducers against the protein and the parasite (determined by ELISA, IFA (Figure 2A) and WB). This also makes them capable of inducing protection against experimental infection in the *Aotus* monkey experimental model (Figure 2B) which has an almost identical immune system to that of humans (C. F. Suarez et al., 2006). Since the Santa Lucia strain gives very weird and irreproducible results (this being the only *Aotus*-adapted *P. falciparum* one), testing Spz-induced immunity means that analysis of Spz-derived mHABPs is limited to determining very high, long-lasting, antibody induction (VHLLAI), as assessed by IFA (Table 1) and WB.
Changes in mHABP secondary structure would include α-helices becoming displaced, shortened or modified as in **22814** (1783) (Table 1) (Cifuentes et al., 2003a), modified β-turns, as in **24246** (3289), **10008** (4044) and **24112** (4044) (Cifuentes et al., 2003b) and when they have random structures they acquire specific conformations, as in **10022** (4313) (distorted type III' turn in T7 to F10) or **23426** (6754) (type V turn between V3-L6) (Purmova et al., 2002; Bermudez et al., 2012) (Table 1).

At the 3D structural level, amino acid replacement induces the formation of characteristic left-handed polyproline II ($PPII_L$)-like structures in some mHABP regions for an appropriate fit into the HLA-DRβ* PBR to allow a bi-molecular HLA-DRβ*-mHABP complex formation to be properly presented to the T-lymphocyte receptor (TCR). These $PPII_L$ helices have their specific structural characteristics, such as 3.1 amino acids (2 to 4) per turn, with 9.2Å per pitch, side chains perpendicular to the peptide's backbone, no intra-, nor inter-chain H-bond formation, backbone angle rotation being ψ (145±25 Å) and φ (-75±25 Å) (Horng and Raines, 2006). The foregoing allows a perfect fit into the HLA-DRβ1* PBR. These mHABPs O and N backbone free electrons pairs establish 9-13 H-bonds with specific atoms of the side chains of conserved residues (Qα9, Sα53, Nα62, Nα69, Wβ61, and some variable residues, such as Kβ74) in MHC-II molecules, establishing 9-11 atom ring structures (Patarroyo et al., 2012a; Patarroyo et al., 2012b) to firmly anchor an mHABP to the HLA-DRβ1* PBR, as elegantly shown by Jardetzky (Jardetzky et al., 1996) .

Throughout these years we have established that most modifications must be made in mHABP unstructured regions (Table 1) and, according to previously published rules, that 2 to 4 replacements are needed to convert such regions into $PPII_L$ structures, thereby facilitating mHABP binding to the HLA-DRβ1* PBR, leaving the rest of the molecule unmodified. This would suggest that mHABPs have both T-cell binding sequences able to interact with the TCR as well as B-cell sequences able to induce antibody production against the whole molecule.

To the best of our knowledge, these are the first structural-functional T- and B-cell epitopes (tailor-made) forming components of a complete, fully protective, anti-*P. falciparum* malaria vaccine, as thoroughly demonstrated (Curtidor et al., 2011; Patarroyo et al., 2011).

Rotamer orientation for appropriate TCR interaction

Once firmly anchored to the HLA-DRβ* PBR via H-bonds, mHABPs have to be presented to the TCR to induce an appropriate immune response. The TCR scans the topochemical characteristics of the HLA-DRβ*-mHABP complex which, due to the peculiar diagonal canonical TCR orientation, allows ±60° freedom (Rudolph et al., 2006). Therefore, mHABP rotamer orientation must ensure their solvent-exposed or upwardly-orientated TCR contacting residues is specific stereo-electronic and topochemical. In pure atomic molecular architecture, the χ1 angles of residues localized in positions p3 and p7 (position is designated by p in the rest of the paragraph) must have *gauche*+ orientation (Table 2) as well as the some χ2 angle in p5, p2 must be polar and orientated towards the right-hand side-chain of an mHABP backbone, p3 must be apolar and towards the left, p5 perpendicular to a peptide's backbone structure, p7 towards the right and p8 towards the left (Bermudez et al., 2014). These physicochemical parameters have allowed the development of principles and rules for a logical and rational methodology for minimal subunit-based, multi-epitope, multi-stage, fully-protective, complete, definitive chemically-synthesised vaccines which can also be used for developing vaccines against other infectious diseases, such as tuberculosis, Ebola, etc., and even cancer associated with or induced by microbes, providing strong support for our functional-structural approach to developing new vaccines.

Most parts of microbes (including malaria), just like Achilles' body, are invulnerable or have many shields or tricks to protect themselves but, like the hero of the Iliad, very small parts of their structure (body/heels) are vulnerable and this is where can be hurt and killed.

Conflict of interest disclosure

"The authors declare no competing financial interest."

References

Ambroggio, X., Jiang, L., Aebig, J., Obiakor, H., Lukszo, J., and Narum, D.L. (2013). The epitope of monoclonal antibodies blocking erythrocyte invasion by Plasmodium falciparum map to the dimerization and receptor glycan binding sites of EBA-175. PloS one *8*, e56326.

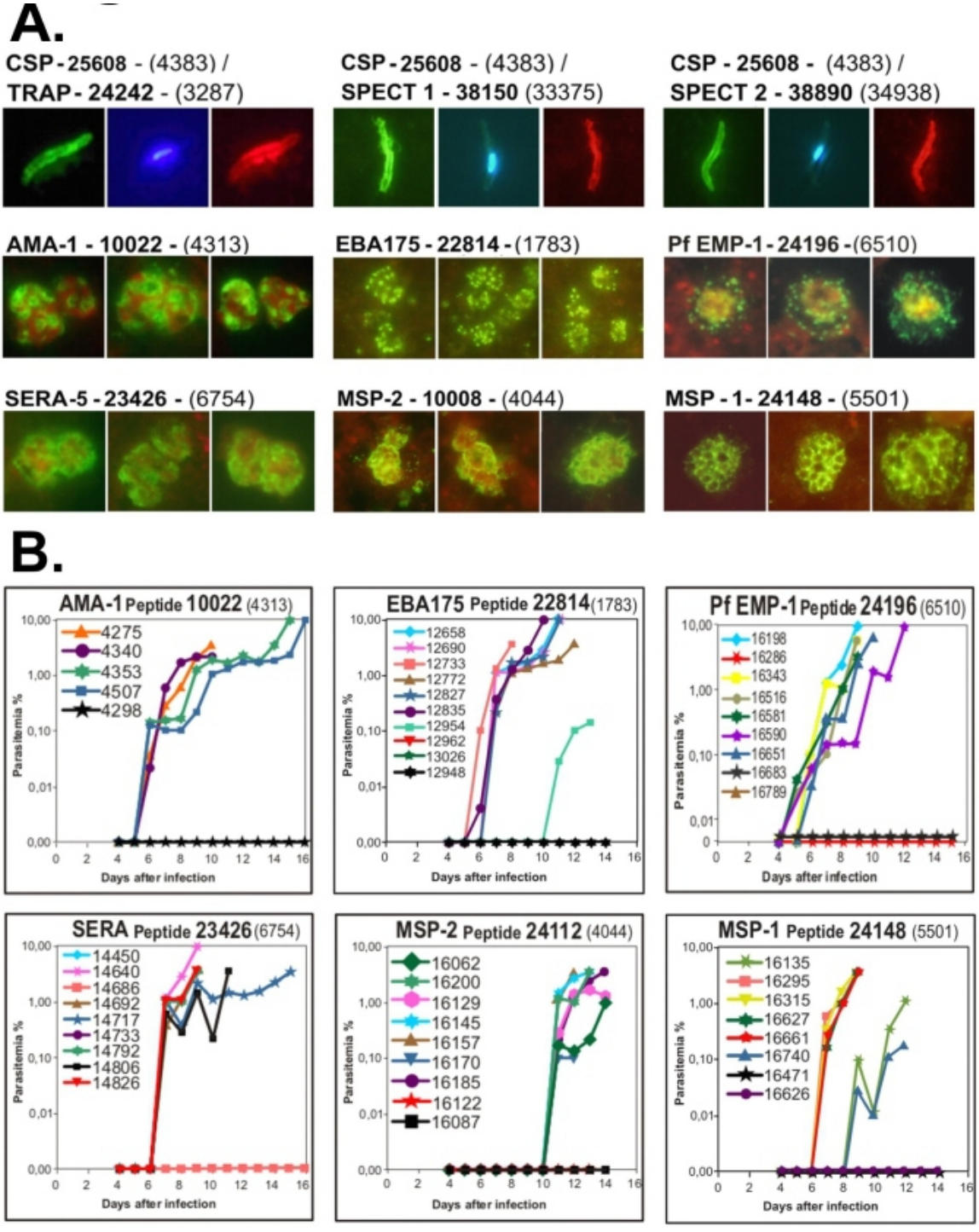

Figure 2. (**A**) Sporozoite and merozoite protein immunofluorescence patterns and location recognized by *Aotus* monkey sera, having high antibody titers when immunized with mHABPs (shown in bold) from corresponding proteins (shown in bold letters) and cHABPs (shown in parentheses). Spz IFA (first row) *Aotus* antibodies against CSP **25608** (4383) were used for these triple-labeling studies as reference, using anti-*Aotus* IgG coupled to fluorescein isothiocyanate (FITC) (showing green fluorescence on Spz membrane). Immune sera reactivity with SPECT-1 and -2 proteins was detected by using anti-*Aotus* IgG coupled to rhodamine (RITC) (showing red under a fluorescence microscope). Nuclear DNA was stained with 4,6-diamidino-2-phenylindole (DAPI) showing bright blue fluorescence. Regarding Mrz protein localization, sera from *Aotus* monkeys immunized with mHABPs (in bold), derived from proteins (also in bold letters), led to corresponding cHABPs (in parentheses) completely agreeing with the localization of the *P. falciparum* proteins from which these mHABPs had been derived. (**B**) This Figure gives some examples of the parasitaemia course in *Aotus* monkeys immunized with fully protection-inducing peptides. The course of parasitaemia displayed on a semi-logarithmic scale was quantified daily by the highly specific and sensitive acridine orange staining method by fluorescence microscope.

Table 2. IMPIPS Φ, ψ and χ1 angles. The colors of residues whose position is horizontally displayed on top follow the code: p1 (fuchsia), p2 (red), p3 (pale blue), p4 (dark blue), p5 (pink), p6 (orange), p7 (grey), p8 (yellow) and p9 (green). The colors displayed in the Table correspond to structure conformations present in these mHABPs: (grey: $PPII_L$), (orange: αR), (lilac: αL). Residues in p3 (dark blue) and p7 (yellow) have *gauche*+ orientation, while χ1 angles (red) have *gauche*− orientation, blocking, interfering or suppressing mHABPs.

Protein/Allele	Position	P1	P2	P3	P4	P5	P6	P7	P8	P9
CSP 25608.37-DRβ1*0401/0402	AA	F	S	L	G	E	N	P	N	A
	ϕ	-77.7	-82.1	-80.6	-91.8	-77.9	-78.4	-46.5	-61.6	61
	Ψ	129	114.9	122.5	85.1	125.5	128.1	149.4	119.8	44.9
	χ_1	-175	-175	-70		-58.4	-174	-7.4	80	
CSP 32958.2 - DRβ1*0401/0402	AA	M	N	N	P	P	N	F	N	V
	ϕ	-75.8	-157	-79.4	-56	-55.5	-159	-137.1	-166	-66.3
	Ψ	-3	79.1	133	127.9	122.4	79.7	42.1	83.1	-32.1
	χ_1	-75.1	-172	-171.9	8.9	8.1	-172	-156.6	-148	104.1
AMA-1 10022.43 - DRβ5*0102/0101	AA	F	H	P	S	G	K	S	P	V
	ϕ	140.2	-129	-62.4	-90.8	-179	-83.7	-137.2	-62.7	-92.4
	Ψ	131.1	108.3	95.5	115.6	-96.4	118	99	127	84.1
	χ_1	-112	-171	-24.7	-173		61.5	-69.8	-24.8	-167
EBA-175 22814.42 - DRβ1*03	AA	M	E	Y	W	K	T	I	K	K
	ϕ	-56.3	-71.8	-65	-70.2	55.1	56.2	-85.6	48.9	67
	Ψ	-46.6	-32.2	-37.4	-50.1	44.5	46.3	-59.2	48.4	87
	χ_1	-95.8	-123	-147	-85.2	-56.1	56.4	-73	67.1	-57.8
EBA-175 13790.46 - DRβ1*0401	AA	Y	G	S	D	D	N	D	D	K
	ϕ	-145	-69	82.4	-85.5	-84	-101	-101.3	-92.8	-84.4
	Ψ	-67.8	-86.9	135.8	65.6	111.6	112.9	97.7	119.2	-10.1
	χ_1	28.5		-43.2	66	-62.5	173	-174.3	-172	85.2
MSP-1 10014.35 - DRβ1*0101	AA	Y	H	V	P	L	A	G	V	Y
	ϕ	-66.3	-150	-105.1	-88.7	-109	73.1	50.8	65.1	36.5
	Ψ	-30.3	88.6	102.5	89.6	16.8	-0.7	48.6	31.2	34.2
	χ_1	63.3	-174	-174.3	22.7	65.4			89.9	85.6
SERA 23426.35 - DRβ1*0403	AA	L	T	G	D	D	T	A	D	L
	ϕ	-118	-96.7	-178.9	62.4	63.2	-149	-163.3	-109	57
	Ψ	55.6	28.4	-75	69.6	66.3	69.3	73.8	27	63.1
	χ_1	-78.8	-169		-173	-176	-49.6		71.6	-64.4
MSP-2 10008.23 - DRβ1*12	AA	F	E	V	N	A	Y	N	M	S
	ϕ	49.9	-116	-95	-125	-146	-53	-67.8	-77.9	-114
	Ψ	-67.4	86.9	74	78.8	-62.2	-50.6	-28.3	159.9	-76.5
	χ_1	66.2	-175	-169.3	-172		-169	-165.9	-60.2	-63.5
MSP-2 24112.39 - DRβ1*0403/0401	AA	Y	N	M	V	I	R	R	S	M
	ϕ	-66.2	-59.4	55.7	-93.8	-80.4	-83.5	-74.6	-86.1	-89.5
	Ψ	-15	-42.5	166.7	87.5	-35.1	111.8	101.9	125.3	114.1
	χ_1	-170	-85	-57.1	-73.9	61.3	-175	-179.2	-176	-173
HRP II 24230.13 - DRβ1*07	AA	L	T	A	A	N	A	M	G	L
	ϕ	-60.3	-66.2	-64.4	-61.9	-51.5	-71.2	-49.6	-65.3	-66.9
	Ψ	-76.8	65.1	89.5	-8.2	-19.6	-37.6	-73.1	-20.5	-52.2
	χ_1	-70.1	18.5			109		-113		113.3
MSP-1 24148.7 - DRβ1*07 (MZT)	AA	L	N	I	S	M	L	Q	T	V
	ϕ	65.4	-71.9	51.0	-63.4	-83.8	-58.2	-54.4	-47.2	-100.9
	Ψ	-48.3	106.3	18.2	-72.9	26.0	-59.4	-32.5	-52.9	175.0
	χ_1	-57.1	61.0	62.9	63.0	75.8	167.2	-94	-60.5	68.3
TRAP 24238.44 - DRβ1*07 (SPZ)	AA	F	H	V	G	T	H	P	A	P
	ϕ	-92.8	-82.7	-68.2	-76.3	-54.7	-96.3	-70.4	-44.9	-71.2
	Ψ	-28.9	-163.1	40.4	-54.7	98.2	154.9	-30.9	149.1	-68.9
	χ_1	-147.2	-133.2	61.3		179.8	58.5	25.7		26.4
AMA-1 13480.29 - DRβ1*1101	AA	F	L	P	S	G	K	S	P	V
	ϕ	-99	-152	-83.4	-154	146.7	-85.2	-117.3	-85.5	-98.8
	Ψ	68.1	116.8	80.2	-83.1	106.9	118.3	103.7	68.8	95
	χ_1	24.5	-174	31.6	-173		71.6	-177.3	32.8	60.7

Bai, T., Becker, M., Gupta, A., Strike, P., Murphy, V.J., Anders, R.F., and Batchelor, A.H. (2005). Structure of AMA1 from Plasmodium falciparum reveals a clustering of polymorphisms that surround a conserved hydrophobic pocket. Proceedings of the National Academy of Sciences of the United States of America *102*, 12736-12741.

Baran, K., Dunstone, M., Chia, J., Ciccone, A., Browne, K.A., Clarke, C.J., Lukoyanova, N., Saibil, H., Whisstock, J.C., Voskoboinik, I., and Trapani, J.A. (2009). The molecular basis for perforin oligomerization and transmembrane pore assembly. Immunity *30*, 684-695.

Bermudez, A., Alba, M.P., Vanegas, M., and Patarroyo, M.E. (2010). 3D structure determination of STARP peptides implicated in P. falciparum invasion of hepatic cells. Vaccine *28*, 4989-4996.

Bermudez, A., Calderon, D., Moreno-Vranich, A., Almonacid, H., Patarroyo, M.A., Poloche, A., and Patarroyo, M.E. (2014). Gauche(+) side-chain orientation as a key factor in the search for an immunogenic peptide mixture leading to a complete fully protective vaccine. Vaccine *32*, 2117-2126.

Bermudez, A., Moreno-Vranich, A., and Patarroyo, M.E. (2012). Protective immunity provided by a new modified SERA protein peptide: its immunogenetic characteristics and correlation with 3D structure. Amino acids *43*, 183-194.

Boddey, J.A., Moritz, R.L., Simpson, R.J., and Cowman, A.F. (2009). Role of the Plasmodium export element in trafficking parasite proteins to the infected erythrocyte. Traffic *10*, 285-299.

Cifuentes, G., Guzman, F., Alba, M.P., Salazar, L.M., and Patarroyo, M.E. (2003a). Analysis of a Plasmodium falciparum EBA-175 peptide with high binding capacity to erythrocytes and their analogues using 1H NMR. Journal of structural biology *141*, 115-121.

Cifuentes, G., Patarroyo, M.E., Urquiza, M., Ramirez, L.E., Reyes, C., and Rodriguez, R. (2003b). Distorting malaria peptide backbone structure to enable fitting into MHC class II molecules renders modified peptides immunogenic and protective. J Med Chem *46*, 2250-2253.

Crosnier, C., Bustamante, L.Y., Bartholdson, S.J., Bei, A.K., Theron, M., Uchikawa, M., Mboup, S., Ndir, O., Kwiatkowski, D.P., Duraisingh, M.T., Rayner, J.C., and Wright, G.J. (2011). Basigin is a receptor essential for erythrocyte invasion by Plasmodium falciparum. Nature *480*, 534-537.

Curtidor, H., Vanegas, M., Alba, M.P., and Patarroyo, M.E. (2011). Functional, immunological and three-dimensional analysis of chemically synthesised sporozoite peptides as components of a fully-effective antimalarial vaccine. Curr Med Chem *18*, 4470-4502.

Chen, L., Xu, Y., Healer, J., Thompson, J.K., Smith, B.J., Lawrence, M.C., and Cowman, A.F. (2014). Crystal structure of PfRh5, an essential P. falciparum ligand for invasion of human erythrocytes. eLife *3*.

Doud, M.B., Koksal, A.C., Mi, L.Z., Song, G., Lu, C., and Springer, T.A. (2012). Unexpected fold in the circumsporozoite protein target of malaria vaccines. Proc Natl Acad Sci U S A *109*, 7817-7822.

Farrand, A.J., LaChapelle, S., Hotze, E.M., Johnson, A.E., and Tweten, R.K. (2010). Only two amino acids are essential for cytolytic toxin recognition of cholesterol at the membrane surface. Proc Natl Acad Sci U S A *107*, 4341-4346.

Garcia, J.E., Puentes, A., and Patarroyo, M.E. (2006). Developmental biology of sporozoite-host interactions in Plasmodium falciparum malaria: implications for vaccine design. Clinical microbiology reviews *19*, 686-707.

Gilbert, R.J., Dalla Serra, M., Froelich, C.J., Wallace, M.I., and Anderluh, G. (2014). Membrane pore formation at protein-lipid interfaces. Trends in biochemical sciences *39*, 510-516.

Hadders, M.A., Beringer, D.X., and Gros, P. (2007). Structure of C8alpha-MACPF reveals mechanism of membrane attack in complement immune defense. Science *317*, 1552-1554.

Hamaoka, B.Y., and Ghosh, P. (2014). Structure of the Essential Plasmodium Host Cell Traversal Protein SPECT1. PloS one *9*, e114685.

Hiss, J.A., Przyborski, J.M., Schwarte, F., Lingelbach, K., and Schneider, G. (2008). The Plasmodium export element revisited. PloS one *3*, e1560.

Hodder, A.N., Malby, R.L., Clarke, O.B., Fairlie, W.D., Colman, P.M., Crabb, B.S., and Smith, B.J. (2009). Structural insights into the protease-like antigen Plasmodium falciparum SERA5 and its noncanonical active-site serine. Journal of molecular biology *392*, 154-165.

Horng, J.C., and Raines, R.T. (2006). Stereoelectronic effects on polyproline conformation. Protein science : a publication of the Protein Society *15*, 74-83.

Jardetzky, T.S., Brown, J.H., Gorga, J.C., Stern, L.J., Urban, R.G., Strominger, J.L., and Wiley, D.C. (1996). Crystallographic analysis of endogenous peptides associated with HLA-DR1 suggests a common, polyproline II-like conformation for bound peptides. Proc Natl Acad Sci U S A *93*, 734-738.

Juillerat, A., Lewit-Bentley, A., Guillotte, M., Gangnard, S., Hessel, A., Baron, B., Vigan-Womas, I., England, P., Mercereau-Puijalon, O., and Bentley, G.A. (2011). Structure of a Plasmodium falciparum PfEMP1 rosetting domain reveals a role for the N-terminal segment in heparin-mediated rosette inhibition. Proc Natl Acad Sci U S A *108*, 5243-5248.

Kanodia, S., Kumar, G., Rizzi, L., Pedretti, A., Hodder, A.N., Romeo, S., and Malhotra, P. (2014). Synthetic peptides derived from the C-terminal 6kDa region of Plasmodium falciparum SERA5 inhibit the enzyme activity and malaria parasite development. Biochimica et biophysica acta *1840*, 2765-2775.

Lin, D.H., Malpede, B.M., Batchelor, J.D., and Tolia, N.H. (2012). Crystal and solution structures of Plasmodium falciparum erythrocyte-binding antigen 140 reveal determinants of receptor specificity during erythrocyte invasion. The Journal of biological chemistry *287*, 36830-36836.

McHenry, A.M., and Adams, J.H. (2006). The crystal structure of P. knowlesi DBPalpha DBL domain and its implications for immune evasion. Trends in biochemical sciences *31*, 487-491.

Mota, M.M., Pradel, G., Vanderberg, J.P., Hafalla, J.C., Frevert, U., Nussenzweig, R.S., Nussenzweig, V., and Rodriguez, A. (2001). Migration of Plasmodium sporozoites through cells before infection. Science *291*, 141-144.

Patarroyo, M.E., Alba, M.P., Curtidor, H., Vanegas, M., Almonacid, H., and Patarroyo, M.A. (2014). Using the PfEMP1 head structure binding motif to deal a blow at severe malaria. PloS One *9*, e88420.

Patarroyo, M.E., Bermudez, A., and Alba, M.P. (2012a). The high immunogenicity induced by modified sporozoites' malarial peptides depends on their phi (phi) and psi (psi) angles. Biochem Biophys Res Commun *429*, 81-86.

Patarroyo, M.E., Bermudez, A., and Patarroyo, M.A. (2011). Structural and immunological principles leading to chemically synthesized, multiantigenic, multistage, minimal subunit-based vaccine development. Chem Rev *111*, 3459-3507.

Patarroyo, M.E., Cifuentes, G., Martinez, N.L., and Patarroyo, M.A. (2010a). Atomic fidelity of subunit-based chemically-synthesized antimalarial vaccine components. Progress in biophysics and molecular biology *102*, 38-44.

Patarroyo, M.E., Cifuentes, G., Pirajan, C., Moreno-Vranich, A., and Vanegas, M. (2010b). Atomic evidence that modification of H-bonds established with amino acids critical for host-cell binding induces sterile immunity against malaria. Biochem Biophys Res Commun *394*, 529-535.

Patarroyo, M.E., Moreno-Vranich, A., and Bermudez, A. (2012b). Phi (Phi) and psi (Psi) angles involved in malarial peptide bonds determine sterile protective immunity. Biochemical and biophysical research communications *429*, 75-80.

Patarroyo, M.E., and Patarroyo, M.A. (2008). Emerging rules for subunit-based, multiantigenic, multistage chemically synthesized vaccines. Accounts of chemical research *41*, 377-386.

Pihlajamaa, T., Kajander, T., Knuuti, J., Horkka, K., Sharma, A., and Permi, P. (2013). Structure of Plasmodium falciparum TRAP (thrombospondin-related anonymous protein) A domain highlights distinct features in apicomplexan von Willebrand factor A homologues. The Biochemical journal *450*, 469-476.

Pizarro, J.C., Chitarra, V., Verger, D., Holm, I., Petres, S., Dartevelle, S., Nato, F., Longacre, S., and Bentley, G.A. (2003). Crystal structure of a Fab complex formed with PfMSP1-19, the C-terminal fragment of merozoite surface protein 1 from Plasmodium falciparum: a malaria vaccine candidate. J Mol Biol *328*, 1091-1103.

Pizarro, J.C., Vulliez-Le Normand, B., Chesne-Seck, M.L., Collins, C.R., Withers-Martinez, C., Hackett, F., Blackman, M.J., Faber, B.W., Remarque, E.J., Kocken, C.H., Thomas, A.W., and Bentley, G.A. (2005). Crystal structure of the malaria vaccine candidate apical membrane antigen 1. Science *308*, 408-411.

Purmova, J., Salazar, L.M., Espejo, F., Torres, M.H., Cubillos, M., Torres, E., Lopez, Y., Rodriguez, R., and Patarroyo, M.E. (2002). NMR structure of Plasmodium falciparum malaria peptide correlates with protective immunity. Biochim Biophys Acta *1571*, 27-33.

Rodriguez, L.E., Curtidor, H., Urquiza, M., Cifuentes, G., Reyes, C., and Patarroyo, M.E. (2008). Intimate molecular interactions of P. falciparum merozoite proteins involved in invasion of red blood cells and their implications for vaccine design. Chem Rev *108*, 3656-3705.

Rudolph, M.G., Stanfield, R.L., and Wilson, I.A. (2006). How TCRs bind MHCs, peptides, and coreceptors. Annu Rev Immunol *24*, 419-466.

Sibley, L.D. (2004). Intracellular parasite invasion strategies. Science *304*, 248-253.

Suarez, C.F., Patarroyo, M.E., Trujillo, E., Estupinan, M., Baquero, J.E., Parra, C., and Rodriguez, R. (2006). Owl monkey MHC-DRB exon 2 reveals high similarity with several HLA-DRB lineages. Immunogenetics *58*, 542-558.

Suarez, J.E., Urquiza, M., Puentes, A., Garcia, J.E., Curtidor, H., Ocampo, M., Lopez, R., Rodriguez, L.E., Vera, R., Cubillos, M., Torres, M.H., and Patarroyo, M.E. (2001). Plasmodium falciparum circumsporozoite (CS) protein peptides specifically bind to HepG2 cells. Vaccine *19*, 4487-4495.

Sultan, A.A., Thathy, V., Frevert, U., Robson, K.J., Crisanti, A., Nussenzweig, V., Nussenzweig, R.S., and Menard, R. (1997). TRAP is necessary for gliding motility and infectivity of plasmodium sporozoites. Cell *90*, 511-522.

Tolia, N.H., Enemark, E.J., Sim, B.K., and Joshua-Tor, L. (2005). Structural basis for the EBA-175 erythrocyte invasion pathway of the malaria parasite Plasmodium falciparum. Cell *122*, 183-193.

Tossavainen, H., Pihlajamaa, T., Huttunen, T.K., Raulo, E., Rauvala, H., Permi, P., and Kilpelainen, I. (2006). The layered fold of the TSR domain of P. falciparum TRAP contains a heparin binding site. Protein Sci *15*, 1760-1768.

Vigan-Womas, I., Guillotte, M., Juillerat, A., Hessel, A., Raynal, B., England, P., Cohen, J.H., Bertrand, O., Peyrard, T., Bentley, G.A., Lewit-Bentley, A., and Mercereau-Puijalon, O. (2012). Structural basis for the ABO blood-group dependence of Plasmodium falciparum rosetting. PLoS pathogens *8*, e1002781.

Wright, K.E., Hjerrild, K.A., Bartlett, J., Douglas, A.D., Jin, J., Brown, R.E., Illingworth, J.J., Ashfield, R., Clemmensen, S.B., de Jongh, W.A., Draper, S.J., and Higgins, M.K. (2014). Structure of malaria invasion protein RH5 with erythrocyte basigin and blocking antibodies. Nature *515*, 427-430.

Yap, A., Azevedo, M.F., Gilson, P.R., Weiss, G.E., O'Neill, M.T., Wilson, D.W., Crabb, B.S., and Cowman, A.F. (2014). Conditional expression of apical membrane antigen 1 in Plasmodium falciparum shows it is required for erythrocyte invasion by merozoites. Cellular microbiology *16*, 642-656.

Zhang, X., Perugini, M.A., Yao, S., Adda, C.G., Murphy, V.J., Low, A., Anders, R.F., and Norton, R.S. (2008). Solution conformation, backbone dynamics and lipid interactions of the intrinsically unstructured malaria surface protein MSP2. Journal of molecular biology *379*, 105-121.